JOURNAL OF VIROLOGY, May 2006, p. 4380–4387 Vol. 80, No. 9
0022-538X/06/$08.00+0 doi:10.1128/JVI.80.9.4380–4387.2006

Base Pairing between the 5′ Half of ε and a *cis*-Acting Sequence, Φ, Makes a Contribution to the Synthesis of Minus-Strand DNA for Human Hepatitis B Virus

Teresa M. Abraham and Daniel D. Loeb*

McArdle Laboratory for Cancer Research, University of Wisconsin Medical School, Madison, Wisconsin 53706

Received 29 November 2005/Accepted 9 February 2006

Synthesis of minus-strand DNA of human hepatitis B virus (HBV) can be divided into three phases: initiation of DNA synthesis, the template switch, and elongation of minus-strand DNA. Although much is known about minus-strand DNA synthesis, the mechanism(s) by which this occurs has not been completely elucidated. Through a deletion analysis, we have identified a *cis*-acting element involved in minus-strand DNA synthesis that lies within a 27-nucleotide region between DR2 and the 3′ copy of DR1. A subset of this region (termed Φ) has been hypothesized to base pair with the 5′ half of ε (H. Tang and A. McLachlan, Virology, 303:199–210, 2002). To test the proposed model, we used a genetic approach in which multiple sets of variants that disrupted and then restored putative base pairing between the 5′ half of ε and Φ were analyzed. Primer extension analysis, using two primers simultaneously, was performed to measure encapsidated pregenomic RNA (pgRNA) and minus-strand DNA synthesized in cell culture. The efficiency of minus-strand DNA synthesis was defined as the amount of minus-strand DNA synthesized per encapsidation event. Our results indicate that base pairing between Φ and the 5′ half of ε contributes to efficient minus-strand DNA synthesis. Additional results are consistent with the idea that the primary sequence of Φ and/or ε also contributes to function. How base pairing between Φ and ε contributes to minus-strand DNA synthesis is not known, but a simple speculation is that Φ base pairs with the 5′ half of ε to juxtapose the donor and acceptor sites to facilitate the first-strand template switch.

Human hepatitis B virus (HBV) infection poses a worldwide health concern with approximately 2 billion people infected, of whom 360 million remain chronically infected (28). Chronic HBV infection greatly increases the risk of developing severe liver diseases such as cirrhosis and hepatocellular carcinoma (2). The World Health Organization estimates that about 500,000 to 700,000 people die each year as a consequence of HBV infection (28). An effective vaccine to prevent HBV infection is available, but it cannot be used to treat already-established infections. The high cost of the vaccine impedes its availability in developing countries, where approximately 5 to 20% of the population is infected. Moreover, treatments for HBV infection, such as alpha interferon therapy and nucleoside analogs, have had limited success, primarily due to acute side effects and drug resistance (6). Because active replication of the virus is necessary for chronic infection, understanding the mechanism of replication should ultimately allow us to control HBV pathogenesis.

HBV belongs to the *Hepadnaviridae* family, which is a family of enveloped, double-stranded DNA viruses that primarily infect liver cells (for reviews, see references 5 and 6). After the virus enters the hepatocyte, the DNA genome is deposited into the nucleus where it is repaired to form covalently closed circular DNA (25). Covalently closed circular DNA is transcribed by host RNA polymerase to make subgenomic RNAs and pregenomic RNA (pgRNA). The X protein and the envelope proteins are translated from the subgenomic RNAs. pgRNA, a terminally redundant molecule, serves as the mRNA for the translation of the capsid subunit, C, and the viral polymerase, P, and as the template for reverse transcription (22).

Within the cytoplasm of the hepatocyte, P binds to an encapsidation signal (ε), a stem-loop structure, at the 5′ end of pgRNA (1, 18). Encapsidation of this ribonucleoprotein complex into nucleocapsids, or core particles, is facilitated by host chaperone proteins (16). Reverse transcription occurs within these core particles. The synthesis of the first-strand or minus-strand DNA can be divided into three phases: initiation, template switch, and elongation. P, serving as the protein primer and reverse transcriptase, uses a bulge within ε to initiate synthesis of the first 3 or 4 nucleotides (nt) of minus-strand DNA (27, 29). At this point, the nascent minus-strand DNA covalently bound to P (7) switches templates to a complementary acceptor site within the 3′ copy of direct repeat sequence 1 (DR1) on pgRNA (20, 24, 26). Elongation of minus-strand DNA resumes from this position. The elongation of minus-strand DNA is accompanied by the degradation of pgRNA by the RNase H activity of P (3, 19). The mechanism(s) by which initiation, template switch, or elongation of minus-strand DNA occurs has not been completely elucidated.

A previous study of HBV has shown that complementarity between the nascent minus-strand DNA and the acceptor site is required for template switch (14). Although complementarity is necessary for first-strand template switch, this alone does not explain the specificity of the template switch. There are 21 putative 5′-UUCA-3′ acceptor sequences within the pgRNA of HBV subtype *ayw*. Yet, nascent minus-strand DNA transfers

* Corresponding author. Mailing address: McArdle Laboratory for Cancer Research, University of Wisconsin Medical School, 1400 University Ave., Madison, WI 53706. Phone: (608) 262-1260. Fax: (608) 262-2824. E-mail: loeb@oncology.wisc.edu.

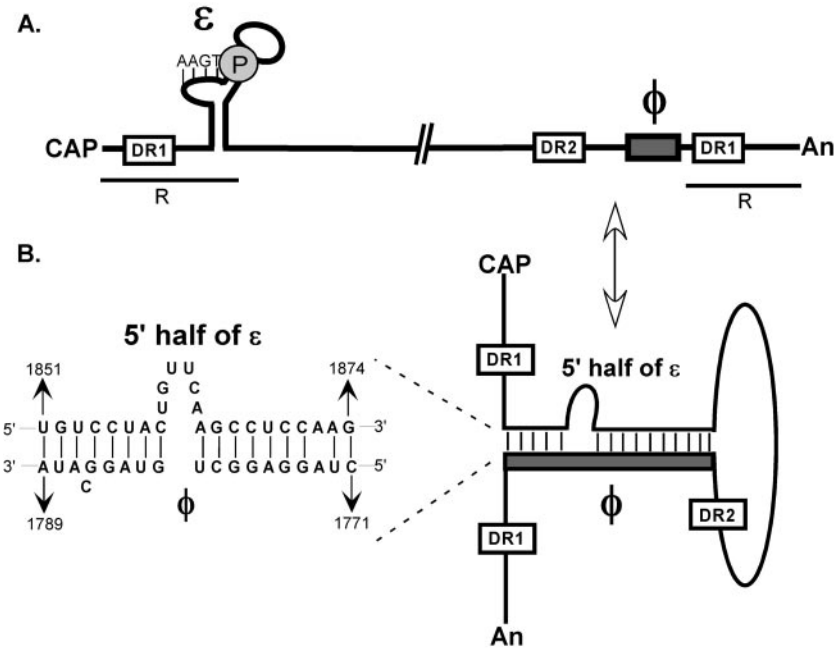

FIG. 1. Model of dynamic conformation of pgRNA during minus-strand DNA synthesis. (A) The location of the *cis*-acting sequence, Φ, between DR2 and the 3′ copy of DR1. Nascent minus-strand DNA covalently linked to the P protein (gray circle) is shown on the bulge of ε, the encapsidation signal. The 5′ end of pgRNA is at nt 1816. The poly(A) tail begins approximately at nt 1930. The 115 nt terminal redundancy of pgRNA is shown by R. (B) A conformation of pgRNA where the 5′ half of ε base pairs with Φ to facilitate minus-strand DNA synthesis. The inset shows the 19 nt of Φ that base pair with the 5′ half of ε. Indicated are the nucleotide coordinates. The left part of the Φ/ε base-paired structure is defined as nucleotides that fall to the left of the bulge of ε. The right part of the Φ/ε base-paired structure is defined as nucleotides that fall to the right of the bulge of ε. The pgRNA is not drawn to scale. DR1, direct repeat sequence 1; DR2, direct repeat sequence 2. ε, encapsidation signal; Φ, *cis*-acting sequence on pgRNA.

efficiently to the authentic acceptor site and not to alternate acceptor sites (9, 14). Therefore, complementarity between the nascent minus-strand and acceptor sequence on the pgRNA is not sufficient for first-strand template switch. Studies of plus-strand DNA synthesis in duck HBV have shown that *cis*-acting sequences are present on minus-strand DNA that contribute to the subsequent plus-strand synthesis (11, 12). It is reasonable to postulate that *cis*-acting sequences are present on pgRNA that facilitate minus-strand DNA synthesis in HBV.

Recently, through deletion analysis, a *cis*-acting sequence that lies between DR2 and the 3′ copy of DR1 on pgRNA was uncovered that was postulated to be involved in minus-strand DNA synthesis (11, 21). Nucleotides within this region (termed Φ) have been hypothesized to base pair with the 5′ half of the encapsidation signal, ε (Fig. 1B) (23). In this report, we show that mutations that disrupt potential base pairing between Φ and the 5′ half of ε reduce levels of minus-strand DNA. More importantly, restoring putative base pairing, albeit with mutant sequences, rescues minus-strand DNA synthesis. Our results are consistent with the idea that base pairing between Φ and the 5′ half of ε makes an important contribution to normal minus-strand DNA synthesis. How base pairing between the two *cis*-acting elements contributes to minus-strand DNA synthesis was not determined, but a simple speculation is that when Φ base pairs with the 5′ half of ε, the donor and acceptor sites on pgRNA are juxtaposed, thereby facilitating the minus-strand template switch.

MATERIALS AND METHODS

Molecular clones. All HBV molecular clones were derived from HBV subtype *ayw* (GenBank accession number V01460). Nucleotide position 1 of HBV subtype *ayw* is the C of the EcoRI site (GAATTC).

The wild-type (WT) HBV reference virus, NL84, expresses HBV pgRNA under the control of the cytomegalovirus immediate early promoter and does not express P, C, X, or surface proteins. NL84 was derived from LJ196 (11) with the following modification: to eliminate the expression of the X protein, the termination codon TAA was introduced into the eighth codon of the X open reading frame by changing C at position 1393 to T (13). The expression plasmid for the HBV replication proteins was LJ96, as described previously (11).

All deletion and substitution mutations were made in the NL84 background, except for deletion mutant 1744-1814, which was made in the LJ196 background. The names of the deletion mutants reflect the deleted nucleotides (inclusive) of the HBV sequences. All mutagenesis was done using a megaprimer protocol (10). The final PCR product was digested with restriction enzymes RsrII and XmaI and cloned into the NL84 plasmid. All mutations were verified by sequencing. Details of molecular cloning will be provided on request.

Cell culture and transfection. Human hepatoma cell line Huh7 was grown in DMEM-F12 supplemented with 5% fetal bovine serum at 37°C in 5% CO_2. DNA transfections were performed using the Ca_2PO_4 precipitation method (15). Huh7 cells were approximately 75% confluent on a 60-mm-diameter plate at the time of transfection. The kinetics of accumulation of encapsidated pgRNA and minus-strand DNA of the WT reference virus were analyzed in Huh7 cells from day 2 to day 8 posttransfection. Primer extension using two primers (dual-PE) for pgRNA and minus-strand DNA showed the amount of minus-strand DNA per encapsidated pgRNA reached a maximum at day 4. Thus, Huh7 cells were harvested on day 4 posttransfection.

Isolation of encapsidated nucleic acid. Viral nucleic acid was harvested from cytoplasmic capsids 4 days posttransfection, as described previously with some modifications (11). Briefly, cells were washed with HEPES-buffered saline plus EGTA buffer (2 mM HEPES, 150 mM NaCl, 0.5 mM EGTA [pH 7.45]) and

frozen at −70°C for at least 1 h. Cells were thawed to room temperature, lysed in 0.5 ml of lysis buffer (0.2% NP-40, 50 mM Tris-HCl [pH 8.0], and 1 mM EDTA) and incubated at 37°C for 10 min. Nuclei were pelleted, and 2 mM $CaCl_2$ and 44 U of micrococcal nuclease (Worthington) were added to the cytoplasmic lysate to digest nonencapsidated nucleic acid and incubated at 37°C for 1.5 h. The cytoplasmic lysate was adjusted to 10 mM EDTA to inactivate micrococcal nuclease. To digest the proteins, 0.4% sodium dodecyl sulfate, 100 mM NaCl, and 0.4 mg of pronase/ml were incubated with the cytoplasmic lysate for 2 h at 37°C. Viral replicative intermediates were extracted once with phenol-chloroform and once with chloroform and stored in ethanol.

Dual-PE. Two end-labeled oligonucleotides, 1948^- and 1661^+, were used to simultaneously detect pgRNA and minus-strand DNA, respectively. Oligonucleotide 1948^- was used to measure pgRNA. This oligonucleotide had sequence complementary to nt 1928 to 1948 on the HBV *ayw* genome and measures pgRNA levels. Oligonucleotide 1661^+ was used to measure minus-strand DNA. This oligonucleotide had sequence complementary to nt 1661 to 1685 on the HBV *ayw* genome and measures minus-strand DNA levels.

Dual-PE analysis was performed on encapsidated nucleic acid isolated from an aliquot equivalent to one-seventh of a transfected plate. Nucleic acids were precipitated, washed with 70% ethanol, and resuspended in 4 μl of H_2O. Approximately 0.8 pmol of each ^{32}P-end-labeled oligonucleotide was added to each reaction. To denature nucleic acids, the reactions were heated at 95°C for 3 min and quenched on wet ice. An incubation step at 50°C for 15 min was done to promote annealing of the oligonucleotide to the viral nucleic acid template. Two units of AMV Reverse Transcriptase (Promega) and final concentrations of 1× AMV Reverse Transcriptase buffer (50 mM Tris-HCl [pH 8.3], 50 mM KCl, 10 mM $MgCl_2$, 0.5 mM spermidine, 10 mM dithiothreitol [Promega]), and 0.2 mM deoxynucleoside triphosphates were added to each reaction tube. Reaction mixtures were incubated at 42°C for 90 min. The reaction conditions described above were empirically determined. HBV plasmid DNA was digested with two restriction enzymes, and primer extension was performed as previously described (8). Primer extension reactions on plasmid DNA controls produced extension products from both primers. The ratio of the amount of product from each primer was used to correct for the efficiency with which each primer was end labeled and the ability to which each primer was able to extend on its template. The primer extension reaction mixtures contained 1× Thermopol buffer [10 mM KCl, 10 mM $(NH_4)_2SO_4$, 20 mM Tris-HCl (pH 8.8), 2 mM $MgSO_4$, 0.1% Triton X-100 (New England Biolabs)], 0.2 mM (each) deoxynucleoside triphosphates, 2 U of Vent exo$^-$ DNA polymerase (New England Biolabs), ~0.8 pmol of end-labeled primer, and 2 ng of digested HBV plasmid DNA. Sequencing ladders were generated using individual primers and HBV plasmid DNA as the template, as described previously (8). Primer extension products were electrophoresed on a 5% denaturing polyacrylamide gel. The gels were dried, exposed onto phosphorimaging cassettes, and scanned using Molecular Dynamics Typhoon (model 8600).

To demonstrate that the amount of minus-strand DNA and pgRNA quantified were directly proportional to the input, serial dilutions of viral nucleic acid were analyzed (data not shown). The efficiency of minus-strand DNA synthesis was determined as the amount of minus-strand DNA divided by the sum of the levels of minus-strand DNA and pgRNA. The efficiency of minus-strand DNA synthesis for each variant was normalized to that of the wild-type reference and expressed as a percentage.

RESULTS

Aim and experimental design. Tang and McLachlan (23) showed that mutating certain nucleotides in the region between nt 1767 and 1794 affected the level of HBV DNA replication. This region lies between DR2 and the 3′ copy of DR1 on pgRNA. In addition, they identified potential base pairing between a subset of this region and the 5′ half of epsilon (Fig. 1). They termed this region phi (Φ). We investigated whether Φ base pairs with ε to contribute to the synthesis of minus-strand DNA.

We used an experimental strategy similar to the one described by Liu et al. (11) to study minus-strand DNA synthesis. The *ayw* subtype of HBV was used for all studies. Briefly, plasmids that expressed mutant pgRNAs (or a WT pgRNA) were cotransfected with a helper plasmid that supplied the replication proteins into Huh7 cells. The pgRNAs expressed from the variant plasmids served as the template for reverse transcription and did not express the replication proteins, due to judiciously placed stop codons. The helper plasmid was competent to express P, C, and X proteins but not surface proteins. The pgRNA expressed from the helper plasmid was defective for RNA encapsidation. Analysis of the WT reference virus indicated that minus-strand DNA accumulation peaked 4 days posttransfection (data not shown). Thus, in our subsequent analyses, cells were harvested 4 days posttransfection.

In our cell culture system, the accumulation of minus-strand DNA for a variant was a function of multiple processes; e.g., transfection of the expression plasmids, cytoplasmic accumulation of pgRNA expressed from the plasmid, encapsidation of pgRNA once in the cytoplasm, and last, the ability of encapsidated pgRNA to be copied into minus-strand DNA. We were interested in evaluating the ability of variant pgRNAs to be copied into minus-strand DNA. Therefore, we could not let variations in the steps prior to minus-strand DNA synthesis influence our analyses. Thus, we needed to determine the level of minus-strand DNA as a function of pgRNA encapsidation events. During the process of replication, encapsidated pgRNA is reverse transcribed to minus-strand DNA. Therefore, only measuring the accumulation of pgRNA-containing capsids will be an incomplete measure of the ability of a virus to encapsidate pgRNA. A measurement of the total number of pgRNA-containing and minus-strand-DNA-containing capsids is a more accurate assessment of the ability of a variant to encapsidate its pregenome. Thus, the ability of a variant to synthesize minus-strand DNA was expressed as a function of the total encapsidation events. To this end, we developed an assay, which we refer to as a dual-PE assay.

The dual-PE assay utilizes two end-labeled oligonucleotides to quantify levels of minus-strand DNA and encapsidated pgRNA simultaneously. A diagram depicting the dual-PE method is shown in Fig. 2. To measure levels of minus-strand DNA, an oligonucleotide that annealed to positions 1661 to 1685 (1661^+) on minus-strand DNA was extended to its 5′ end (nt 1825). To measure pgRNA levels, an oligonucleotide that annealed to positions 1928 to 1948 (1948^-) on the pgRNA was extended to its 5′ end (nt 1816). Oligonucleotide 1948^- also annealed to plus-strand DNA species of duplex linear (DL) and relaxed circular (RC) DNA. Since DL DNA has the same 5′ end as pgRNA, the two products were indistinguishable. The contribution of DL DNA is 3%, whereas the contribution of pgRNA is 97% of the signal in the 132-nt product designated pgRNA/DL. Because the contribution of DL DNA to the pgRNA/DL signal was small, we considered the pgRNA/DL signal to accurately reflect the level of pgRNA in our samples. Oligonucleotide 1948^- annealed to plus-strand DNA of RC and extended to its 5′ end, resulting in a product (366 nt) that was larger than seen for pgRNA and minus-strand DNA. Thus, primer extension products are of different lengths: 132 nt for pgRNA/DL and 165 nt for minus-strand DNA (Fig. 2).

***cis*-acting element for minus-strand DNA synthesis lies within nucleotides 1767 and 1793.** The sequence element Φ is postulated to lie within nt 1771 and 1789 (23). To determine whether Φ is the only sequence within this region to make a

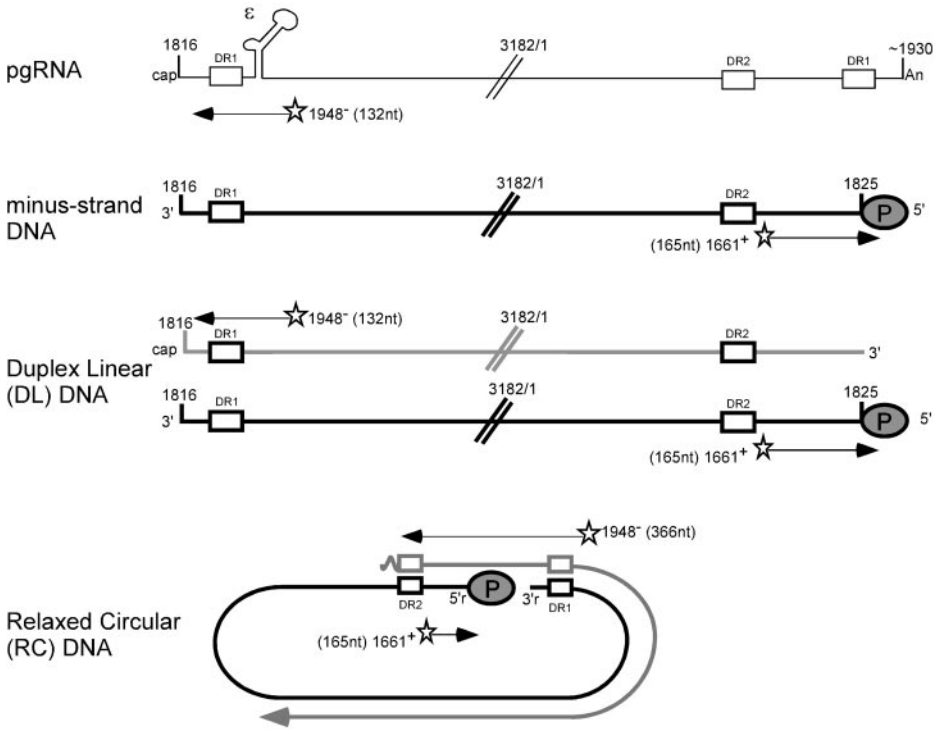

FIG. 2. Schematic representation of dual-PE assay. pgRNA is depicted by a thin dark line, with its salient features and nucleotide positions of the 5′ and 3′ ends indicated. Minus-strand DNA is depicted by a thick dark line, and plus-strand DNA is depicted by a gray line. The P protein covalently linked to the 5′ end of minus-strand DNA is illustrated as a gray oval. The stars represent end-labeled primers. Oligonucleotide 1948^{-} anneals to position 1948 on the pgRNA. AMV reverse transcriptase extends to the 5′ end of pgRNA, resulting in a 132-nt product. Oligonucleotide 1948^{-} also anneals to plus-strand DNA at position 1948^{-}. In the case of DL, it results in a 132-nt product, which comigrates with pgRNA. In the case of RC, extension of oligonucleotide 1948^{-} results in a 366-nt product. Oligonucleotide 1661^{+} anneals at position 1661 on minus-strand DNA and extends to the 5′ end, resulting in a 165-nt product.

contribution to minus-strand DNA synthesis (21), we made and analyzed three deletions: one that deleted nucleotides in the Φ region and two others that deleted ~25 nt either upstream or downstream of Φ. The locations of the deletion variants with respect to the HBV pgRNA are depicted in Fig. 3A. The phenotypes of the deletion variants were determined by the dual-PE assay. Deletion of the sequence between nt 1767 and 1793 resulted in a fourfold reduction in the level of minus-strand DNA, as shown in Fig. 3C. Further, the regions flanking nt 1767 to 1793 did not result in a reduction in the level of minus-strand DNA (Fig. 3C). These results demonstrated that the *cis*-acting sequence lies between nt 1767 to 1793. A subset of this region contains the element described as Φ.

Base pairing in the right half of the putative Φ/ε secondary structure contributes to efficient minus-strand DNA synthesis. To determine whether base pairing between Φ and the 5′ half of ε contributes to function, we asked whether disrupting and then restoring potential base pairs would affect function. A prediction is that if these sequences contribute via base pairing, then disrupting the base pairs will reduce minus-strand DNA levels compared to a WT reference. Subsequent restoration of base pairing, albeit with mutant sequences, is predicted to rescue minus-strand DNA to levels higher than those of the single mutants. We disrupted potential base pairing by making independent mutations on Φ and ε. Potential base pairing between Φ and ε was restored, albeit with mutant sequences, in a third variant. In addition, we utilized the third type of base pairing in RNA, between G and U, to make substitutions in Φ alone that would either disrupt or maintain base pairing. Thus, several sets of variants were analyzed. For ease of description of the variants and their phenotypes, we placed them into three groups.

The first group consisted of three sets of variants that rescued minus-strand DNA levels when potential base pairing between Φ and 5′ half of ε was restored or maintained (Φ1ε1, Φ2ε2, and Φ3Φ4) (Fig. 4A). The mutations in ε1 have been described previously and only change nucleotides in the left side of the ε stem-loop structure (17). The mutations in ε2 only change nucleotides on the left side of the stem-loop structure. ε1 has a fivefold reduction in encapsidation efficiency, whereas the encapsidation efficiency of ε2 is similar to the WT reference (data not shown). Three nucleotides were substituted to their Watson-Crick partner in the Φ1ε1 set. Two nucleotides were substituted to their Watson-Crick partner in the Φ2ε2 set. Nucleotide substitutions in Φ3Φ4 set were designed to either disrupt base pairing in variant Φ3 or maintain base pairing in variant Φ4 by using the third type of base pairing found in RNA between G and U. The ability of these variants to make minus-strand DNA was determined by the dual-PE assay (Fig. 4B). Disrupting putative base pairing (ε1, Φ1, ε2, Φ2, and Φ3) reduced the level of minus-strand DNA synthesized compared

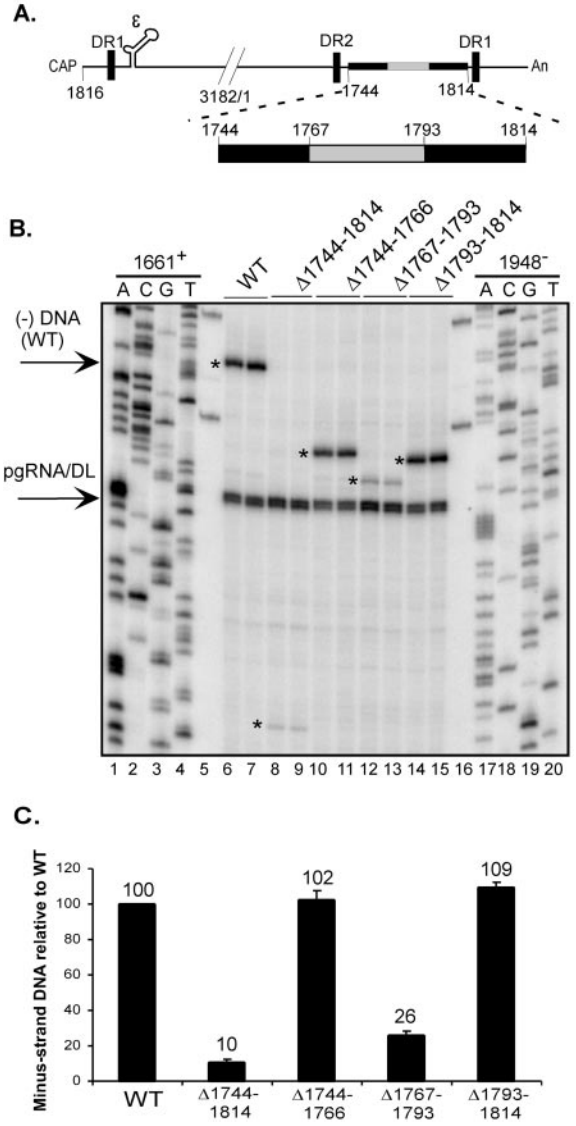

FIG. 3. Deletion analysis between nt 1744 to 1814 defines boundaries of *cis*-acting sequence for minus-strand DNA synthesis. (A) The positions of the deletion variants are indicated on the pgRNA. Φ is located between nt 1767 and 1793. A total of 23 nt was deleted upstream of Φ, and 21 nt were deleted downstream of Φ. (B) Dual-PE analysis of pgRNA and minus-strand DNA levels of deletion variants shown in panel A. The asterisks indicate the positions at which the 5′ ends of minus-strand DNA for the WT and the deletion variants migrate. Because the deletions were located downstream of where oligonucleotide 1661^+ annealed to minus-strand DNA, primer extension reactions resulted in products that reflect the size of the deletion. The positions of 5′ ends of pgRNA and minus-strand DNA (WT) are indicated by arrows on the left. Lanes 1 to 4 and 17 to 20, sequencing ladder of WT HBV DNA; 5 and 16, plasmid DNA control; 6 and 7, WT; 8 and 9, Δ1744-1814; 10 and 11, Δ1744-1766; 12 and 13, Δ1767-1793; 14 and 15, Δ1793-1814. (C) Efficiency of minus-strand DNA synthesis relative to a WT reference. The encapsidation competency of a virus is defined as the sum of pgRNA and minus-strand DNA. Therefore, the ability of a virus to synthesize minus-strand DNA is determined as the level of minus-strand DNA normalized to the sum of pgRNA and minus-strand DNA levels. The efficiency of minus-strand DNA synthesis for each variant was normalized to that of the WT standard. The numbers above each bar indicate the mean values of minus-strand DNA synthesis. The error bars represent standard deviations from analysis of replicative intermediates isolated from at least six independent transfections of each variant.

to the WT reference (Fig. 4C). Although the magnitudes of defects for the single mutants were not as great as the deletion variant spanning 1767 to 1793, all were statistically significant. More importantly, the variants that restored the predicted base pairing between Φ and ε, synthesized minus-strand DNA to levels significantly higher than each of the constituent single variants (the largest P values were <0.01) (Fig. 4C). Therefore, the results for these three sets of variants support the idea that Φ and ε base pair with each other to contribute to minus-strand DNA synthesis.

Not all proposed base pairs are required for minus-strand DNA synthesis. The second group of variants targeted ε and Φ sequences in the left part, as depicted in Fig. 5A, of the Φ/ε base-paired secondary structure. This set consisted of mutations on either ε or Φ that disrupted putative base pairing and a third variant that combined the single mutations to restore the predicted base pairing. The mutations in ε5 lie within the lower stem of ε and have been studied previously (17). Since base pairing in the lower stem of ε is necessary for encapsidation, substitutions were made such that base pairing in this region was maintained. This variant encapsidates pgRNA at an efficiency comparable to that of the WT reference (data not shown). Dual-PE results indicated that variant Φ5 had a slight defect in minus-strand DNA synthesis (75% of the WT level) (Fig. 5C). Importantly, variant ε5 had close to wild-type levels of minus-strand DNA (109% of the WT). The double mutant Φ5/ε5 mimicked the defect in Φ5 (77% of the WT). These results indicate that base pairing between the targeted nucleotides on the left side of the putative ε/Φ base-paired structure does not contribute to function. Thus, not all of the 17 potential base pairs form to contribute to function. In addition, the results are consistent with the idea either that the nucleotides targeted in variant Φ5 make a small contribution to the synthesis of minus-strand DNA or that these particular substitutions are tolerated by the virus.

Base pairing between Φ and ε is not sufficient for minus-strand DNA synthesis. In the third group, the variants intended to restore potential base pairing (Φ6/ε6, Φ7/ε7, Φ8/ε8, and Φ10) did not make minus-strand DNA to levels significantly higher than the variants that disrupted potential base pairing (Fig. 6A). This phenotype was displayed by four sets of variants analyzed by dual-PE (Fig. 6B). Variant set Φ6ε6 mutated 4 nt to their Watson Crick partners. Mutations in ε6 have been described previously (17). In addition, another set of variants, Φ7ε7, which has a permutation of mutations made in set Φ6ε6, was analyzed. The substitutions in ε6 and ε7 were made such that base pairing in the upper part of the upper stem-loop structure of ε was maintained. These variants displayed a fivefold reduction in encapsidation efficiency (data not shown). Variant set Φ8ε8 changed 3 nt in the same position as the Φ1ε1 set, and variant ε8 displayed a fivefold reduction in pgRNA encapsidation efficiency (data not shown). The fourth set of variants disrupted base pairing between Φ and ε by mutating nucleotides on Φ alone (Φ9) and restored base pairing (Φ10) by utilizing the third type of base pairing found in RNA, between G and U (Fig. 6A).

The results demonstrated that variants designed to disrupt potential base pairs (ε6, Φ6, ε7, Φ7, ε8, Φ8, and Φ9) made reduced levels of minus-strand DNA. Additionally, the variants that were predicted to restore base pairing between the 5′

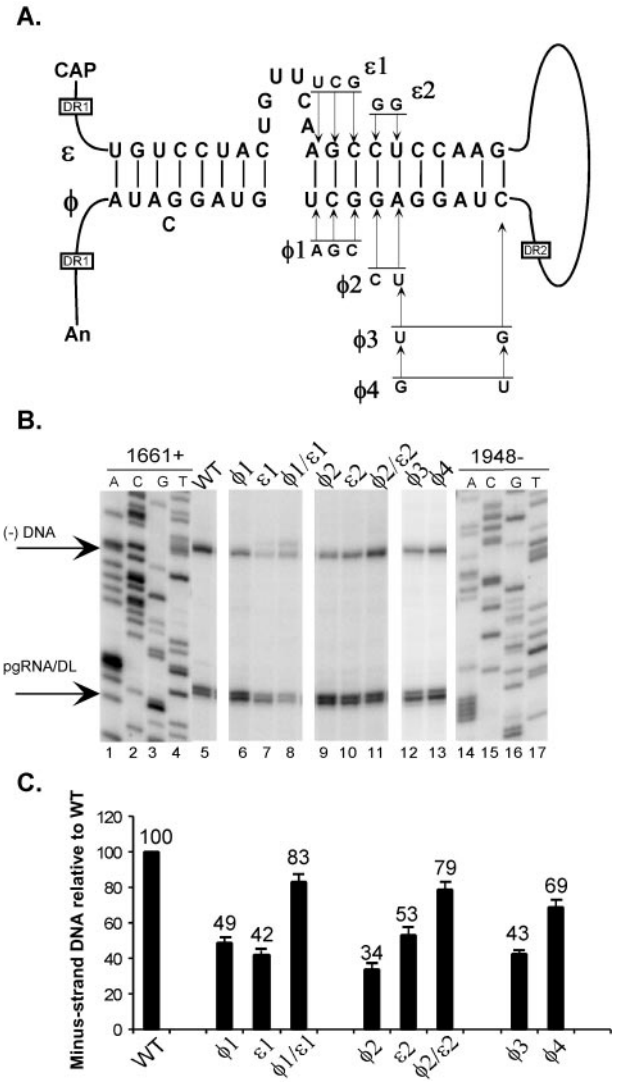

FIG. 4. Base pairing between Φ and 5′ half of ε contributes to minus-strand DNA synthesis. (A) Putative base pairing between 19 nt of Φ and the 5′ half of ε on the pgRNA. Substitutions designed to disrupt base pairing are shown. Variants that restore base pairing combine the corresponding ε and Φ substitutions. Variants Φ3 and Φ4 change nucleotides on Φ alone. The positions of the DR sequences on pgRNA are indicated. The diagram is not drawn to scale. (B) Dual-PE assay of pgRNA and minus-strand DNA levels of substitution variants shown in panel A. The position of the 5′ ends of pgRNA and minus-strand DNA are indicated by arrows on the left. Lanes 1 to 4 and 14 to 17, sequencing ladders generated from WT HBV DNA; 5, WT; 6, Φ1; 7, ε1; 8, Φ1/ε1; 9, Φ2; 10, ε2; 11, Φ2/ε2; 12, Φ3; 13, Φ4. (C) The efficiency of minus-strand DNA synthesis was calculated by dividing the level of minus-strand DNA by the sum of minus-strand DNA plus pgRNA. The denominator represents the total encapsidation events. The numbers above each bar indicate the mean values of minus-strand DNA synthesis. The error bars indicate standard deviations from analysis of replicative intermediates isolated from at least six independent transfections of each variant.

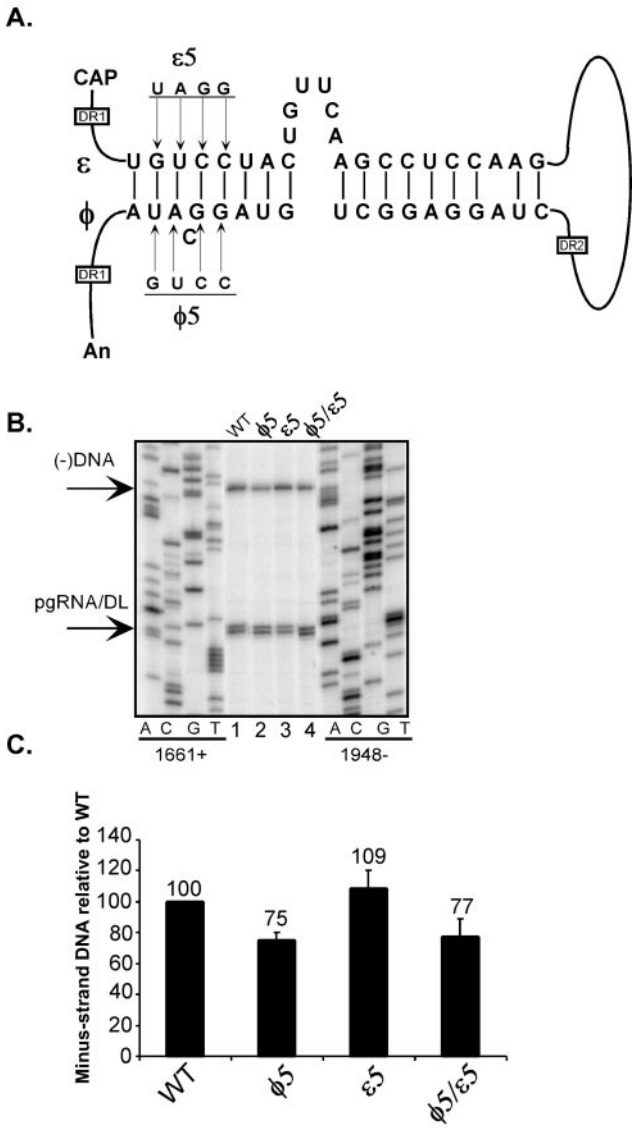

FIG. 5. The left part of Φ does not base pair with ε to contribute to minus-strand DNA synthesis. (A) Putative base pairing between Φ and the 5′ half of ε. Nucleotide substitutions that disrupt base pairing are indicated. Variants that restore base pairing combine the corresponding ε and Φ substitutions. (B) Dual-PE assay of pgRNA and minus-strand DNA levels of substitution variants shown in panel A. The positions of the 5′ ends of minus-strand DNA and pgRNA are indicated by arrows on the left. Sequencing ladders generated from WT HBV DNA, using individual primers, are indicated. Lanes 1, WT; 2, Φ5; 3, ε5; 4, Φ5/ε5. (C) Graphic representation of the amount of minus-strand DNA normalized to the total encapsidation events. The numbers above each bar indicate the mean values of minus-strand DNA synthesis. The error bars indicate standard deviations from analysis of replicative intermediates isolated from at least six independent transfections of each variant.

half of ε and Φ also made reduced levels of minus-strand DNA (Fig. 6B, lanes 6, 9, 12, and 15). These data suggest a requirement for the specific sequence within the Φ/ε base-paired structure. Data from four independent sets of variants were consistent with this interpretation.

DISCUSSION

Our test of the base pairing model proposed by Tang and McLachlan (23) shows that at least a subset of the nucleotides on Φ base pairs with ε contribute to minus-strand DNA synthesis. Mutations that impair putative base pairing between Φ and the 5′ half of ε reduce levels of minus-strand DNA,

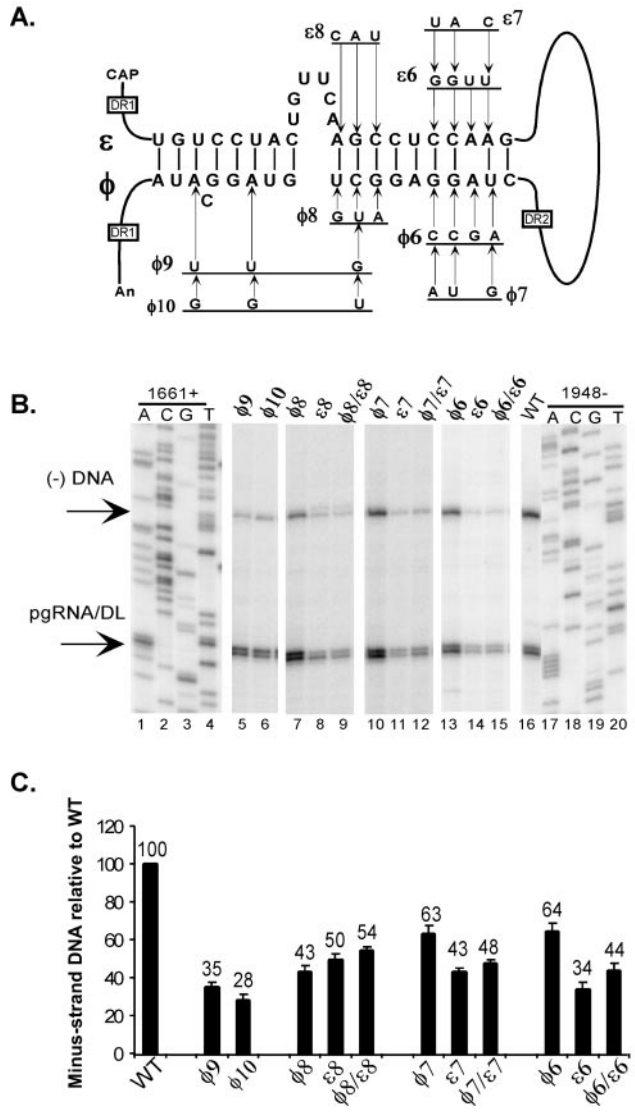

FIG. 6. Base pairing between Φ and the 5′ half of ε is not sufficient for minus-strand DNA synthesis. (A) Putative base pairing between Φ and the 5′ half of ε on pgRNA is shown. Nucleotide substitutions that disrupt base pairing are indicated. Variants that restore base pairing combine the corresponding ε and Φ substitutions. Variants Φ9 and Φ10 only mutate nucleotides on Φ. (B) Dual-PE assay of pgRNA and minus-strand DNA levels of substitution variants shown in part A. The positions of the 5′ end of minus-strand DNA and pgRNA are indicated by arrows on the left. Lanes 1 to 4 and 17 to 20, sequencing ladders generated from WT HBV DNA; 5, Φ9; 6, Φ10; 7, Φ8; 8, ε8; 9, Φ8/ε8; 10, Φ7; 11, ε7; 12, Φ7/ε7; 13, Φ6; 14, ε6; 15, Φ6/ε6; 16, WT. (C) Graphic representation of the amount of minus-strand DNA normalized to the total encapsidation events. The numbers above each bar indicate the mean values of minus-strand DNA synthesis. The error bars indicate standard deviations from analysis of replicative intermediates isolated from at least six independent transfections of each variant.

whereas compensatory mutations restore minus-strand DNA levels (Fig. 4). Exactly how these base pairs contribute to minus-strand DNA synthesis is unclear. One speculation is that Φ base pairs with the 5′ half of ε to juxtapose the donor and acceptor sites to facilitate a first-strand template switch. Although our data are consistent with this interpretation, it does not rule out other possibilities. Besides the template switch, there are two additional stages at which the Φ/ε base-paired structure may function: initiation of nascent minus-strand DNA and elongation of minus-strand DNA after the template switch. It is possible that the Φ/ε base-paired structure contributes to initiation of minus-strand DNA. Analysis of the Ty1 retrotransposon of yeast shows that a long-range interaction between the 5′ and 3′ ends of the RNA makes an important contribution to the early steps of replication, such as initiation of DNA synthesis (4).

The secondary structure ε plays a crucial role in the encapsidation process. The P protein binds to ε, and this ribonucleoprotein complex is encapsidated. In addition, the bulge of ε serves as the site of initiation of minus-strand DNA. We have shown that base pairing between the 5′ half of ε and Φ contributes to minus-strand DNA synthesis. Therefore, the nucleotides in the 5′ half of ε participate in two exclusive secondary structures. This duality raises questions as to when and how the ε stem-loop structure is dissolved and the Φ/ε base-paired structure is formed. Does initiation of minus-strand DNA synthesis require the formation of the Φ/ε base-paired structure, or does the Φ/ε base-paired structure form after initiation of nascent minus-strand DNA? Does P protein play a role in formation of the Φ/ε base-paired structure? Currently, we do not know at which phase the Φ/ε base-paired structure functions.

Our results suggest that not all potential base pairs between ε and Φ contribute to the synthesis of minus-strand DNA. Data from one set of mutations (ε5) indicate that changing nucleotides on the 5′ half of ε does not affect function, but changing nucleotides on Φ affects minus-strand DNA synthesis slightly (Fig. 5). It is possible that the mutations made in variant Φ5 are well tolerated and lead to a less-severe reduction in levels of minus-strand DNA. It is unclear at this time as to how this portion of the Φ sequence contributes to function.

Some variants with double mutations (Φ6/ε6, Φ7/ε7, and Φ8/ε8) did not have minus-strand DNA levels that were significantly higher than their constituent single mutations. We think these results suggest a sequence requirement within the Φ/ε secondary structure. Such a sequence requirement could be due to a protein(s) within the capsid that recognizes a specific sequence to facilitate minus-strand DNA synthesis. Or it could reflect that these sequences contribute to a favorable conformation of pgRNA that is important for efficient minus-strand DNA synthesis. Other interpretations of the Φ6ε6, Φ7ε7, and Φ8ε8 variant sets are more ambiguous. The lack of robust restoration of minus-strand DNA levels could be argued to indicate that the putative base pairing does not contribute to function. But the converse interpretation is also plausible. The individual mutations within the aforementioned sets reduce minus-strand DNA levels two- to threefold. If these mutations were to act separately to influence viral replication, minus-strand DNA levels might be expected to be reduced approximately four- to ninefold with the double mutations. Because this was not the case, it could be argued that replication function was partially restored by the complementary base pairing with the Φ6ε6, Φ7ε7, and Φ8ε8 variants. As complete function was not restored by complementary sequences in all cases, the nucleotide sequence also appears to contribute to the level of minus-strand DNA synthesis.

Interestingly, mutations such as those in Φ1/ε1 are tolerated and lead to a restoration of function, but mutations such as those in Φ8/ε8, although in the same position as Φ1/ε1, do not result in restoration of minus-strand DNA synthesis. Why this might be the case is uncertain. One possible explanation is that an alternate base-paired structure, different from the preferred one, may form in the Φ8/ε8 double mutant, thus leading to inefficient minus-strand DNA synthesis.

Further, we noticed a band at least 1 to 2 nt longer than the expected 5′ end of minus-strand DNA when mutations were made in the region immediately downstream of the bulge of ε (Fig. 4B and 6B). The alternate 5′ end of minus-strand DNA was not seen when mutations were made immediately downstream of ε1 or ε8 (see ε2 and Φ2/ε2 in Fig. 4B). We verified that the band was a product of an extension from minus-strand DNA and not an aberrant plus-strand nucleic acid product by performing primer extension with oligonucleotide 1661^+ alone (data not shown). We do not think that the extra band is an artifact resulting from the specific identity of the mutant sequences, because ε8, a version of mutations in ε1, also displays the extra band. Sequences surrounding the bulge are predicted to contribute to specificity of the priming reaction (14). Our observations could be explained if the mutations in ε1 and ε8 affected the specificity of the location of priming of minus-strand DNA by P. Alternatively, the additional 5′ ends of the minus-strand DNA for ε1 and ε8 could be due to an aberrant template switch to a noncanonical acceptor site. Again, we do not have the experimental means to distinguish whether the mutations affected priming or template switch of minus-strand DNA.

Using a genetic approach, we have gained insight into whether the *cis* elements Φ and ε contribute to minus-strand DNA synthesis by base pairing. Our results are consistent with the idea that base pairing between Φ and ε contributes to function, but the mechanism by which the Φ/ε base-paired structure functions remains unknown. Our results are also consistent with the idea that Φ/ε base pairing is necessary but not sufficient for efficient minus-strand DNA synthesis. But the mechanism by which the primary sequence of Φ and/or ε contributes to minus-strand DNA synthesis is not known. Additionally, putative base-paired structures between Φ and ε regions have been proposed for other mammalian and avian hepadnaviruses (23). The question as to whether this is a common mechanism among all hepadnaviruses to facilitate the synthesis of minus-strand DNA remains to be established.

ACKNOWLEDGMENTS

We thank Lauren M. Nettenstrom and John P. Maufort for help in constructing some molecular clones. We thank members of the Loeb laboratory for helpful discussions. We also thank Bill Sugden for critically reviewing the manuscript.

This work was supported by National Institutes of Health grant CA22443.

REFERENCES

1. **Bartenschlager, R., and H. Schaller.** 1992. Hepadnaviral assembly is initiated by polymerase binding to the encapsidation signal in the viral RNA genome. EMBO J. **11:**3413–3420.
2. **Beasley, R. P.** 1988. Hepatitis B virus: the major etiology of hepatocellular carcinoma. Cancer **61:**1942–1956.
3. **Chen, Y., and P. Marion.** 1996. Amino acids essential for RNase H activity of hepadnaviruses are also required for efficient elongation of minus-strand viral DNA. J. Virol. **70:**6151–6156.
4. **Cristofari, G., C. Bampi, M. Wilhelm, F.-X. Wilhelm, and J.-L. Darlix.** 2002. A 5′-3′ long-range interaction in Ty1 RNA controls its reverse transcription and retrotransposition. EMBO J. **21:**4368–4379.
5. **Ganem, D., and R. Schneider.** 2001. *Hepadnaviridae*: the viruses and their replication, p. 2923–3036. *In* D. M. Knipe, P. M. Howley, D. E. Griffin, R. A. Lamb, M. A. Martin, B. Roizman, and S. E. Straus (ed.), Fields virology, 4th ed. Lippincott Williams & Wilkins, Philadelphia, Pa.
6. **Ganem, D., and A. M. Prince.** 2004. Hepatitis B virus infection—natural history and clinical consequences. N. Engl. J. Med. **350:**1118–1129.
7. **Gerlich, W., and W. Robinson.** 1980. Hepatitis B virus contains protein attached to the 5′ terminus of its complete DNA strand. Cell **21:**801–809.
8. **Habig, J. W., and D. D. Loeb.** 2002. Small DNA hairpin negatively regulates in situ priming during duck hepatitis B virus reverse transcription. J. Virol. **76:**980–989.
9. **Ho, T.-C., K.-S. Jeng, C.-P. Hu, and C. Chang.** 2000. Effects of genomic length on translocation of hepatitis B virus polymerase-linked oligomer. J. Virol. **74:**9010–9018.
10. **Ke, S., and E. Madison.** 1997. Rapid and efficient site-directed mutagenesis by single-tube 'megaprimer' PCR method. Nucleic Acids Res. **25:**3371–3372.
11. **Liu, N., L. Ji, M. L. Maguire, and D. D. Loeb.** 2004. *cis*-acting sequences that contribute to the synthesis of relaxed-circular DNA of human hepatitis B virus. J. Virol. **78:**642–649.
12. **Liu, N., R. Tian, and D. D. Loeb.** 2003. Base pairing among three *cis*-acting sequences contributes to template switching during hepadnavirus reverse transcription. Proc. Natl. Acad. Sci. USA **100:**1984–1989.
13. **Melegari, M., P. P. Scaglioni, and J. R. Wands.** 1998. Cloning and characterization of a novel hepatitis B virus x binding protein that inhibits viral replication. J. Virol. **72:**1737–1743.
14. **Nassal, M., and A. Rieger.** 1996. A bulged region of the hepatitis B virus RNA encapsidation signal contains the replication origin for discontinuous first-strand DNA synthesis. J. Virol. **70:**2764–2773.
15. **Okayama, H., and C. Chen.** 1987. High-efficiency transformation of mammalian cells by plasmid DNA. Mol. Cell. Biol. **7:**2745–2752.
16. **Park, S. G., S. M. Lee, and G. Jung.** 2003. Antisense oligodeoxynucleotides targeted against molecular chaperonin Hsp60 block human Hepatitis B virus replication. J. Biol. Chem. **278:**39851–39857.
17. **Pollack, J., and D. Ganem.** 1993. An RNA stem-loop structure directs hepatitis B virus genomic RNA encapsidation. J. Virol. **67:**3254–3263.
18. **Pollack, J., and D. Ganem.** 1994. Site-specific RNA binding by a hepatitis B virus reverse transcriptase initiates two distinct reactions: RNA packaging and DNA synthesis. J. Virol. **68:**5579–5587.
19. **Radziwill, G., W. Tucker, and H. Schaller.** 1990. Mutational analysis of the hepatitis B virus P gene product: domain structure and RNase H activity. J. Virol. **64:**613–620.
20. **Rieger, A., and M. Nassal.** 1996. Specific hepatitis B virus minus-strand DNA synthesis requires only the 5′ encapsidation signal and the 3′-proximal direct repeat DR1. J. Virol. **70:**585–589.
21. **Shin, M.-K., J. Lee, and W.-S. Ryu.** 2004. A novel *cis*-acting element facilitates minus-strand DNA synthesis during reverse transcription of the hepatitis B virus genome. J. Virol. **78:**6252–6262.
22. **Summers, J., and W. S. Mason.** 1982. Replication of the genome of a hepatitis B-like virus by reverse transcription of an RNA intermediate. Cell **29:**403–415.
23. **Tang, H., and A. McLachlan.** 2002. A pregenomic RNA sequence adjacent to DR1 and complementary to epsilon influences hepatitis B virus replication efficiency. Virology **303:**199–210.
24. **Tavis, J., S. Perri, and D. Ganem.** 1994. Hepadnavirus reverse transcription initiates within the stem-loop of the RNA packaging signal and employs a novel strand transfer. J. Virol. **68:**3536–3543.
25. **Tuttleman, J., C. Pourcel, and J. Summer.** 1986. Formation of the pool of covalently closed circular viral DNA in hepadnavirus-infected cells. Cell **47:**451–460.
26. **Wang, G., and C. Seeger.** 1993. Novel mechanism for reverse transcription in hepatitis B viruses. J. Virol. **67:**6507–6512.
27. **Wang, G., and C. Seeger.** 1992. The reverse transcriptase of the hepatitis B virus acts as a protein primer for viral DNA synthesis. Cell **71:**663–670.
28. **World Health Organization.** 2004. Hepatitis B vaccines. Wkly. Epidemiol. Rec. **79:**255–263.
29. **Zoulim, F., and C. Seeger.** 1994. Reverse transcription in hepatitis B viruses is primed by a tyrosine residue of the polymerase. J. Virol. **68:**6–13.